ANL-HEP-PR-79-17

Comparison of Jet Size in $\bar{\nu}p$ INTERACTIONS WITH With That in e^+e^- Annihilation

MASTER

by

M. Derrick, A. Fridman, P. Gregory, F. Lopinto, B. Musgrave,
J. Schlereth, P. Schreiner and R. Singer
S.J. Barish, R. Brock, A. Engler, T. Kikuchi, R.W. Kraemer,
F. Messing, B.J. Stacey and M. Tabak
V.E. Barnes, D.D. Carmony, E. Fernandez,
A.F. Garfinkel and A.T. Laasanen

DISCLAIMER

This book was prepared as an account of work sponsored by an agency of the United States Government. Neither the United States Government nor any agency thereof, nor any of their employees, makes any warranty, express or implied, or assumes any legal liability or responsibility for the accuracy, completeness, or usefulness of any information, apparatus, product, or process disclosed, or represents that its use would not infringe privately owned rights. Reference herein to any specific commercial product, process, or service by trade name, trademark, manufacturer, or otherwise, does not necessarily constitute or imply its endorsement, recommendation, or favoring by the United States Government or any agency thereof. The views and opinions of authors expressed herein do not necessarily state or reflect those of the United States Government or any agency thereof.

ARGONNE NATIONAL LABORATORY, ARGONNE, ILLINOIS

Operated under Contract W-31-109-Eng-38 for the
U. S. DEPARTMENT OF ENERGY

The submitted manuscript has been authored by a contractor of the U. S. Government under contract No. W-31-109-ENG-38. Accordingly, the U. S. Government retains a nonexclusive, royalty-free license to publish or reproduce the published form of this contribution, or allow others to do so, for U. S. Government purposes.

ANL-HEP-PR-79-17

Comparison of Jet Size in $\bar{\nu}p$ Interactions With That in e^+e^- Annihilation

M. DERRICK, A. FRIDMAN*, P. GREGORY+, F. LOPINTO, B. MUSGRAVE, J. SCHLERETH, P. SCHREINER, and R. SINGER
Argonne National Laboratory, Argonne, IL 60439

S. J. BARISH, R. BROCK, A. ENGLER, T. KIKUCHI, R. W. KRAEMER, F. MESSING, B. J. STACEY, and M. TABAK
Carnegie-Mellon University, Pittsburgh, PA 15213

V. E. BARNES, D. D. CARMONY, E. FERNANDEZ, A. F. GARFINKEL, and A. T. LAASANEN
Purdue University, W. Lafayette, IN 47907

Abstract

Using new $\bar{\nu}p$ charged-current data from the Fermilab 15-foot hydrogen bubble chamber, some properties of the $\bar{\nu}$-induced hadronic jets are studied. The angular size of the jets is measured and compared with results from e^+e^- annihilation. The jets in the two processes are found to be quite similar in terms of the variables sphericity, thrust, and energy flow.

*On leave from CEA, Saclay, France.
+Present Address: CERN, EP Division, Geneva 23, Switzerland.

Data on e^+e^- annihilation [1-5] in the c.m. energy range $3 < W < 13$ GeV have recently been compared fairly successfully with fragmentation jet models and Quantum Chromodynamics (QCD) jet theories. However, it has been suggested [6-8] that in the QCD framework, due to gluon emission, the single quark jet (the current fragments) produced in lepton-nucleon (ℓN) collisions has different properties than the jets produced in e^+e^- collisions, while the jet resulting from the recoiling quark-quark system (the target fragments) will likely be more collimated than that of the single quark. Of course, in the naive quark parton model (QPM), a fragmenting single quark jet of a certain flavor is expected to be the same in e^+e^- and ℓN interactions. In both of these models for ℓN collisions, one is also faced with the complication of the primordial transverse momentum of the confined quarks in the nucleon. It therefore seems very important to experimentally compare the properties of jets in ℓN and e^+e^- collisions.

In this paper we present new $\bar{\nu} p$ charged-current data and show that the observed jets are in fact very similar in angular size and shape to those found in e^+e^- experiments for center-of-mass energies $W \lesssim 10$ GeV. We also examine the direction in which the measured jet axis actually points in $\bar{\nu} p \to \mu^+ X^o$ events at finite energy.

The data sample was obtained from exposures of the Fermilab 15-foot hydrogen bubble chamber to a broad-band antineutrino beam. Over 90% of the data were obtained using 400 GeV protons with focussing provided by two magnetic horns. Data from neutrino-induced "background" events in the experiment were also analyzed and are displayed in some of the distributions in this paper. Only events with three or more charged particles were processed. Neutral particles are in general not detected in this experiment, so one must make some assumptions to calculate the beam energy [9]. The muon track was selected using kinematic techniques [10]. Corrections have been made in all distributions for muon selection efficiency, neutral current background, and energy resolution.

Since published results on e^+e^- jets are always given for events having $\geq$ 4 charged particles, we impose the selection $\geq$ 5 charged particles ($\geq$ 4 charged hadrons) on our data. To reduce background, we also demand that $y = (E_{\bar{\nu}} - E_{\mu})/E_{\bar{\nu}} \leq 0.8$. We use only events with $E_{\bar{\nu}} > 5$ GeV. We present the jet results in the c.m. frame of the virtual boson-nucleon system, as suggested by Stevenson [6]. We do not impose a Q^2 selection on the data presented in this paper, but have checked that a $Q^2 > 1$ $(\mathrm{GeV}/c)^2$ selection has little effect on our results for $W \geq 3$ GeV.

The angular size of a jet has been defined by many different variables. We first consider sphericity [11-12], defined as

$$S = \frac{3}{2} \,\mathrm{Min} \sum_i (P_\perp^2)_i / \sum_i (P^2)_i \quad ,$$

where $P_\perp$ is relative to the jet axis and the sum is over all charged particles. For a "perfect" jet event, $S \to 0$. The jet axis $\hat{S}$ is defined as the direction in space that minimizes S; for $\bar{\nu}p$ interactions, that axis should approach the virtual boson-nucleon axis at high c.m. energy.

A second measure of the shape of an event is the variable thrust [13-14], defined as

$$T = \mathrm{Max} \left[\sum_i |P_\parallel|_i / \sum_i (P)_i \right] \quad ,$$

where $P_\parallel$ is relative to the jet axis and the sum is over all charged particles. For a "perfect" jet event, $T \to 1$. The jet's thrust axis, $\hat{T}$, is the direction that maximizes T. At high energy, one expects $\hat{T} = \hat{S}$ and so it is of interest to check how close these two directions are at present energies.

In calculating S and T, we use tracks from both the single quark and quark-quark hemispheres. Figure 1(a-b) shows our measurements of $\langle S \rangle$ and $1 - \langle T \rangle$ as a function of hadronic mass, W, from 2 to ~ 11 GeV. Both $\bar{\nu}p$ and νp data are plotted. Above 4 GeV, there is a clear decrease in the jet angular size as the hadronic mass increases. The variation is consistent with a $(\log W)^{-1}$ dependence. There is little difference between the jets of the two lepton-proton reactions. Also shown are uncorrected e^+e^- annihilation measurements for a similar W range [2-5], including the new results from PETRA. Very similar jets are produced by e^+e^- and $\bar{\nu}p$ interactions. This is quite surprising considering that the $\bar{\nu}p$ events always contain a baryon and the e^+e^- data contain a large charm particle contribution for W above 4 GeV.

Figure 1(c) shows $\langle S \rangle$ for $\bar{\nu}p$ as a function of W for different particle multiplicities. As one would expect, low multiplicity events are more jet-like than those of high multiplicity at a fixed W. However, above 4 GeV, all topologies show a decrease in $\langle S \rangle$ with increasing mass.

In Fig. 2 we compare the shapes of the $\frac{1}{\sigma}\frac{d\sigma}{dS}$ distributions in e^+e^- [2,5] and $\bar{\nu}p$ interactions for two mean values of W. The agreement between the e^+e^- data and the ℓN data is again quite good. Both sets of data show a clear dip for $S \lesssim 0.1$.

We next study the question of where the jet axis determined by sphericity or thrust actually points. In Fig. 3(a-f), we show the angular distribution between the "natural" jet axis $\hat{Q}$ defined by the virtual boson-nucleon direction and the $\hat{S}$ and $\hat{T}$ axes. For $2.5 \leq W \leq 3.0$ GeV, the jet direction is approximately isotropically distributed with respect to $\hat{Q}$. Only for $W \gtrsim 4.5$ GeV does the jet axis defined by $\hat{S}$ or $\hat{T}$ appear to be a meaningful concept - i.e., strongly correlated with the virtual boson direction. This conclusion is consistent with the data of Fig. 1 that show $\langle S \rangle$ decreasing with increasing W only above 4 GeV. In all remaining distributions in this paper, a $W \geq 4.5$ GeV selection has been made.

The theoretical uncertainty in the direction of the jet axis can also be measured by calculating the angle θ between the $\hat{S}$ and $\hat{T}$ axis. For the two mass ranges $4.5 \leq W \leq 5.5$ GeV and $5.5 \leq W \leq 12$ GeV, $\langle \theta_{(\hat{S}\cdot\hat{T})} \rangle = 14.5^\circ \pm 0.9^\circ$ and $10.7^\circ \pm 0.7^\circ$, respectively. These values are essentially identical to those found [3] in e^+e^- annihilation at 9.4 GeV. The strong correlation between the jet axis and the direction $\hat{P}_F$ of the fastest particle observed in e^+e^- reactions is also evident in $\bar{\nu}p$ interactions. For $5.5 \leq W \leq 12$ GeV, $\langle \theta(\hat{S}\cdot\hat{P}_F) \rangle = 11.3^\circ \pm 0.8^\circ$ and $\langle \theta(\hat{T}\cdot\hat{P}_F) \rangle = 19.5^\circ \pm 0.9^\circ$, so that the difference between the sphericity axis and the direction of the fastest particle is not larger, within errors, than the difference between the directions of the sphericity and thrust axes.

Another measure of the angular size of the jet is given by the energy flow of the particles with respect to the jet axis. Fig. 4(a) shows the distribution of $\frac{1}{W}\frac{dE_C}{d\lambda}$, where λ is the angle relative to the thrust axis of a charged particle with energy E_C. The distribution is given for particles in both the single quark and quark-quark hemispheres, defined by a plane perpendicular to the thrust axis. The selections $W > 4.5$ GeV and $T > 0.85$ have been applied. The shapes of the jets in the two hemispheres are indistinguishable, with $\langle \lambda \rangle_q = 28^\circ \pm 2^\circ$ and $\langle \lambda \rangle_{qq} = 26^\circ \pm 2^\circ$. It has been suggested that the quark-quark jet might in fact be narrower than the single quark jet [15]. We find no evidence for this hypothesis for $W \lesssim 10$ GeV. Fig. 4(b) displays the strong negative correlation which exists between $\langle \lambda \rangle$ and T in both $\bar{\nu}p$ and e^+e^- reactions.[3] The data for the two processes are at somewhat different energies, but the results are consistent, again showing that the jets are of very similar size.

In summary, we have found that the concept of a jet is meaningful only for values of hadronic mass $\geqslant 4.5$ GeV, the uncertainty in the direction of the jet axis is $\sim 10^{\circ}$, and that the angular size of jets in charged-current $\bar{\nu}p$ interactions is almost identical to that found in e^+e^- annihilation. The overall similarity between the ℓN and e^+e^- data in Figs. 1, 2, and 4 implies that the transverse momentum of the quarks within the proton does not increase the width of the jets.

This experiment was made possible by the support of the Neutrino Department at Fermilab and by the operating crew of the 15-foot bubble chamber. This research was supported by the U. S. Department of Energy.

References

1. R. F. Schwitters et al., Phys. Rev. Letters 35 (1975) 1320.
2. G. Hansen et al., Phys. Rev. Letters 35 (1975) 1609.
3. C. Berger et al., Phys. Letters 78B (1978) 176.
4. C. Berger et al., Phys. Letters 81B (1979) 410.
5. R. Brandelik et al., Phys. Letters 83B (1979) 261.
6. P. M. Stevenson, Nucl. Phys. B150 (1979) 357.
7. J. Ranft and G. Ranft, Phys. Letters 82B (1979) 129.
8. P. Binetruy and G. Girardi, TH2611 - CERN preprint (1979).
9. S. J. Barish et al., Phys. Rev. D18 (1978) 2205.
10. E. Fernandez, A. Garfinkel, A. T. Laasanen, Purdue University Report PU79-480 (unpublished).
11. J. D. Bjorken and S. J. Brodsky, Phys. Rev. D1, (1970) 1416.

12. S. Brandt and H. Dahmen, Z. Physik C1 (1979) 61.

13. S. Brandt et al., Phys. Letters 12 (1969) 57.

14. E. Farhi, Phys. Rev. Letters 39 (1977) 1587.

15. P. M. Stevenson, Imperial College preprint ICTP/78-79/16.

Figure Captions

Fig. 1 (a) $1 - \langle T \rangle$ as a function of hadronic mass W for $\bar{\nu}p$, νp, and e^+e^- interactions.

(b) $\langle S \rangle$ as a function of hadronic mass W for $\bar{\nu}p$, νp, and e^+e^- interactions.

(c) $\langle S \rangle$ as a function of n_c in $\bar{\nu}p$ and νp interactions.

Fig. 2 $\frac{1}{\sigma}\frac{d\sigma}{dS}$ distributions: (a) $\bar{\nu}p$ for $\langle W \rangle = 6.6$ GeV and e^+e^- for $W = 7$ GeV, and (b) $\bar{\nu}p$ plus νp for $\langle W \rangle = 10.5$ GeV and e^+e^- for $W = 13$ GeV.

Fig. 3 The angular distributions between the $\vec{Q} = \vec{P}_{\bar{\nu}} - \vec{P}_{\mu^+}$ vector and the $\hat{S}$ and $\hat{T}$ vectors for three ranges of W in $\bar{\nu}p$ interactions.

Fig. 4 (a) $\frac{1}{W}\frac{dE_C}{d\lambda}$ distributions for $\bar{\nu}p$ interactions with $W > 4.5$ GeV and $T \geq 0.85$. The solid curve represents the single quark data and the dotted curve represents the quark-quark data.

(b) Correlation between the width of the energy flow distribution of 4(a) and the value of thrust of $\bar{\nu}p$ and e^+e^- interactions.

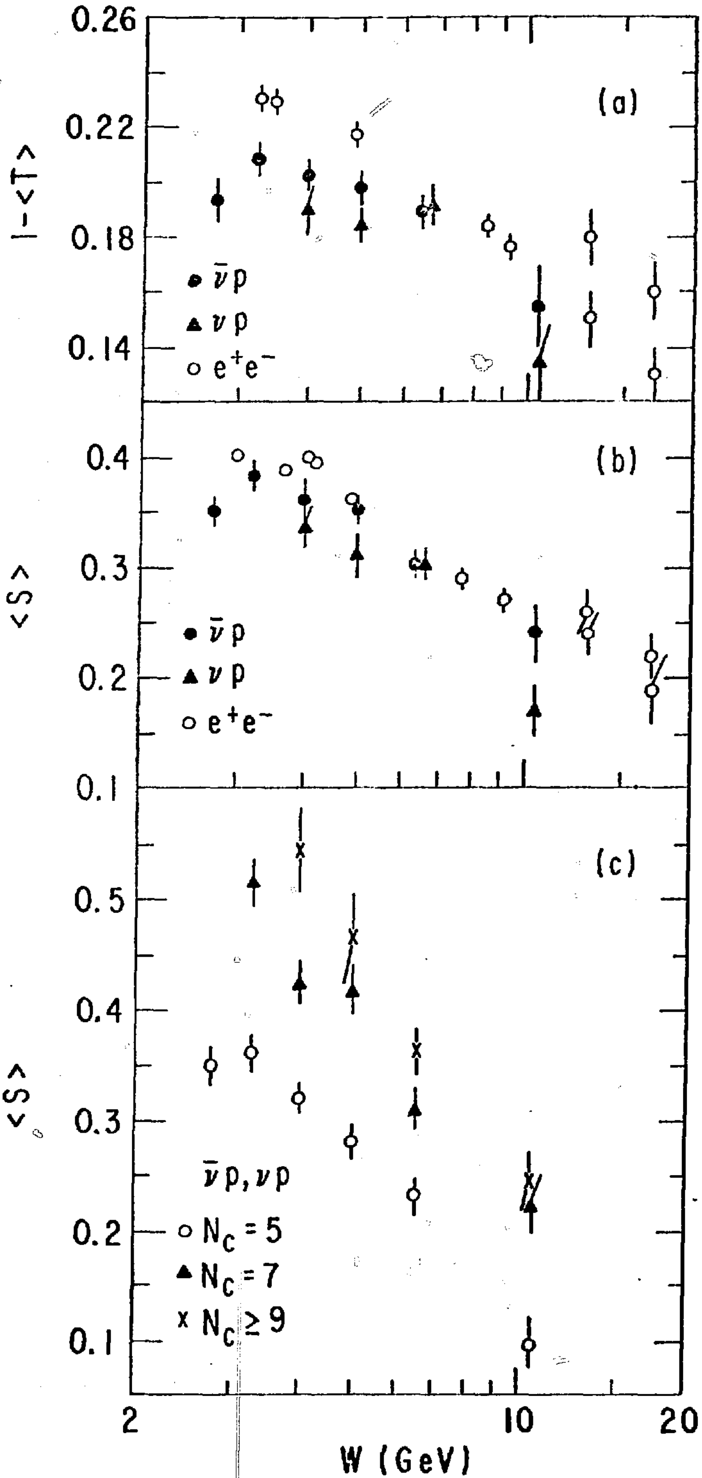

0.26
0.22
0.18
0.14
1-<T>
(a)
$\bar{\nu}$p
νp
e+e−
0.4
0.3
0.2
0.1
<S>
(b)
$\bar{\nu}$p
νp
e+e−
0.5
0.4
0.3
0.2
0.1
<S>
(c)
$\bar{\nu}$p, νp
$N_c = 5$
$N_c = 7$
$N_c \geq 9$
2
10
20
W (GeV)

Fig. 1

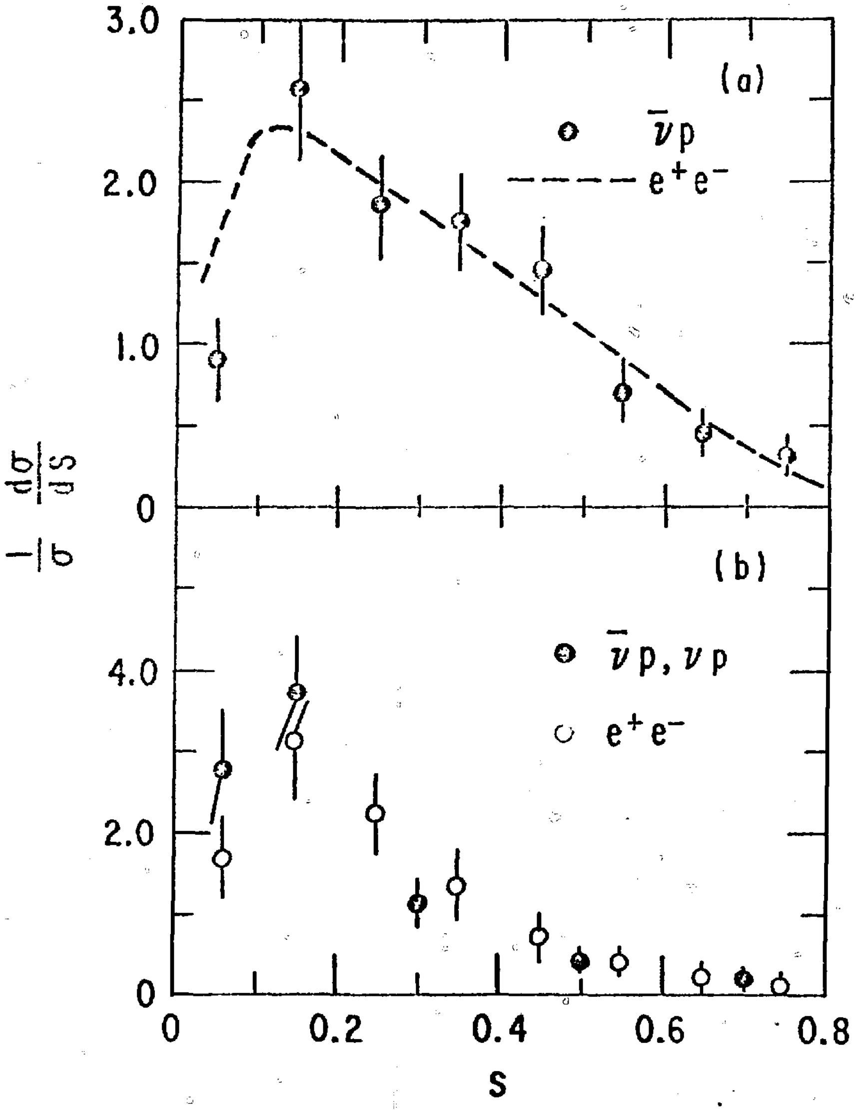
3.0
2.0
1.0
0
4.0
2.0
0
(a)
$\bar{\nu}$p
e^+e^-
(b)
$\bar{\nu}$p, νp
e^+e^-
$\frac{1}{\sigma}\frac{d\sigma}{dS}$
0
0.2
0.4
0.6
0.8
S

Fig. 2

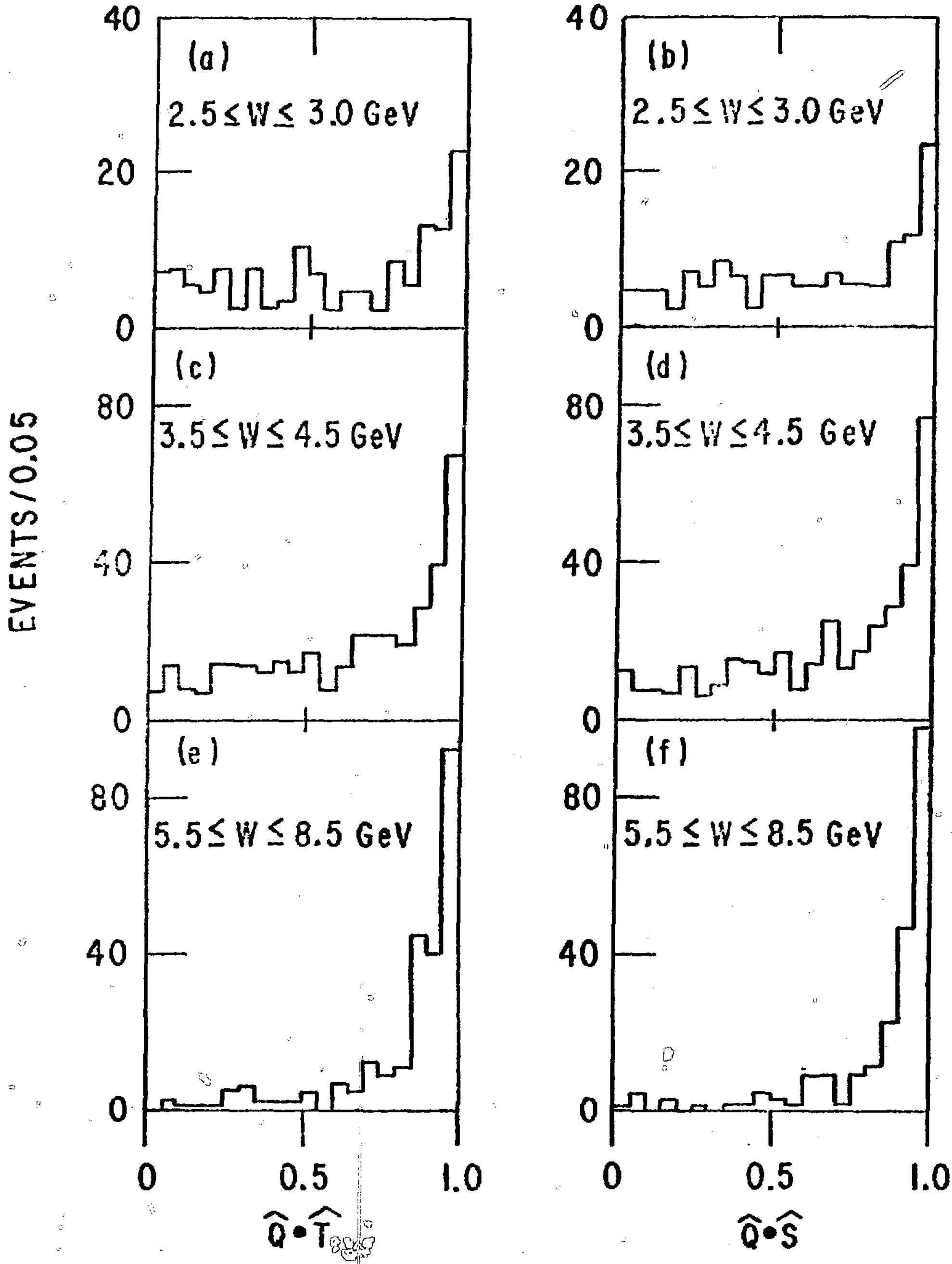

EVENTS/0.05
(a)
2.5 ≤ W ≤ 3.0 GeV
(b)
2.5 ≤ W ≤ 3.0 GeV
(c)
3.5 ≤ W ≤ 4.5 GeV
(d)
3.5 ≤ W ≤ 4.5 GeV
(e)
5.5 ≤ W ≤ 8.5 GeV
(f)
5.5 ≤ W ≤ 8.5 GeV
Q̂•T̂
Q̂•Ŝ

Fig. 3

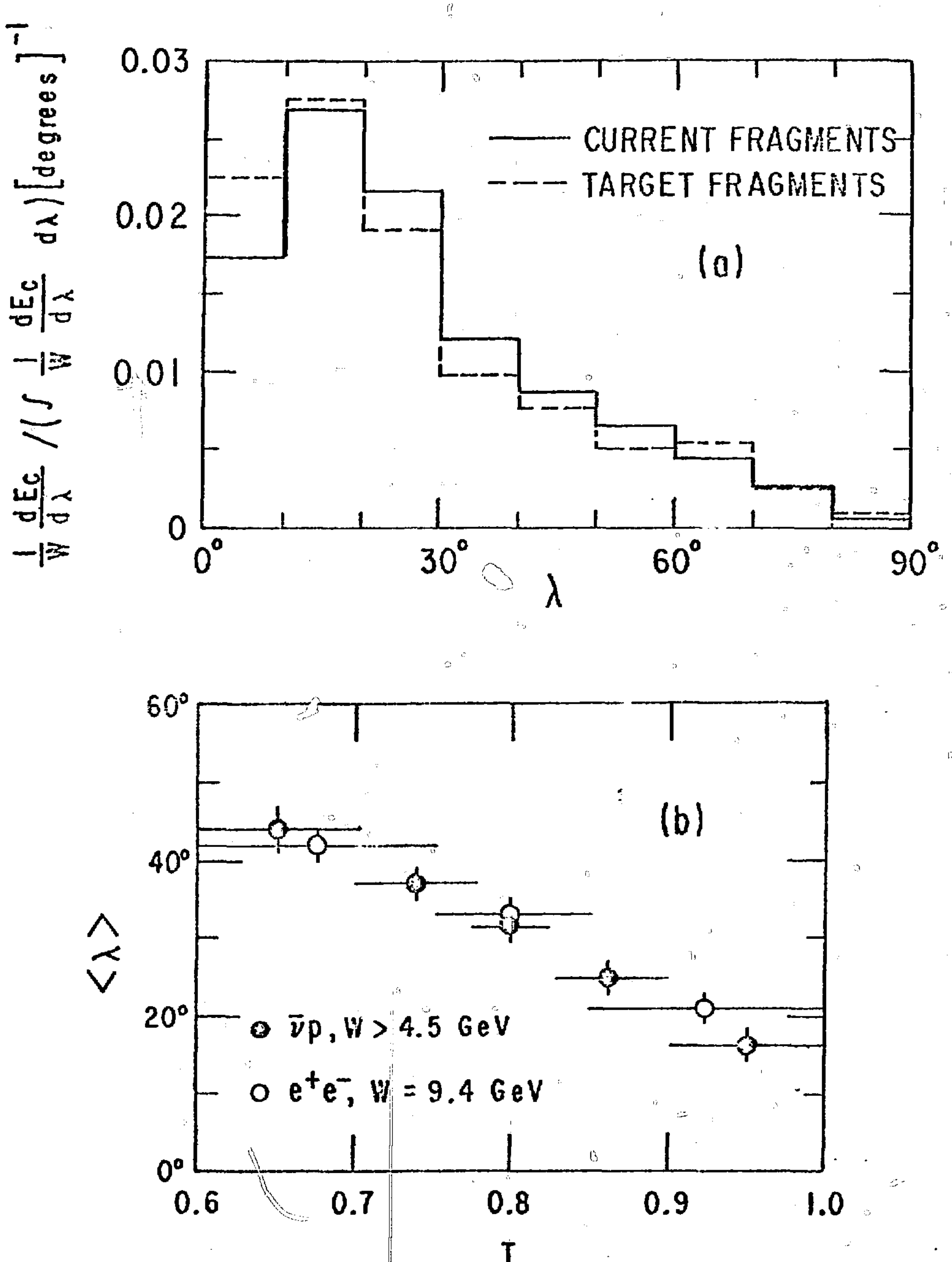

0.03
0.02
0.01
0
0°
30°
60°
90°
λ
CURRENT FRAGMENTS
TARGET FRAGMENTS
(a)
60°
40°
20°
0°
0.6
0.7
0.8
0.9
1.0
T
⟨λ⟩
(b)
ν̄p, W > 4.5 GeV
e+e−, W = 9.4 GeV

Fig. 4